Peer-reviewed version available at *Int. J. Adv. Manuf. Technol.* **2019**; doi:10.1007/s00170-019-04794-9

Inverse analysis of the residual stress in laser–assisted milling

Yixuan Feng[1,*], Tsung-Pin Hung[2], Yu-Ting Lu[3], Yu-Fu Lin[3], Fu-Chuan Hsu[3], Chiu-Feng Lin[3], Ying-Cheng Lu[3] and Steven Y. Liang[1]

[1]Woodruff School of Mechanical Engineering, Georgia Institute of Technology, Atlanta, United States
[2]Department of Mechanical Engineering, Cheng Shiu University, Kaohsiung, Taiwan
[3]Metal Industries Research and Development Centre (MIRDC), Kaohsiung, Taiwan

Keywords:

Inverse analysis; Iterative gradient search; Laser-assisted milling; Residual stress; Ti-6Al-4V

Correspondence to:

Yixuan Feng: yfeng82@gatech.edu

Abstract In laser-assisted milling, higher temperature in shear zone softens the material potentially resulting in a shift of mean residual stress, which significantly affects the damage tolerance and fatigue performance of product. In order to guide the selection of laser and cutting parameters based on the preferred mean residual stress, inverse analysis is conducted by predicting residual stress based on guessed process parameters, which is defined as the forward problem, and applying iterative gradient search to find process parameters for next iteration, which is defined as the inverse problem. An analytical inverse analysis is therefore proposed for the mean residual stress in laser-assisted milling. The forward problem is solved by analytical prediction of mean residual stress after laser-assisted milling. The residual stress profile is predicted through the calculation of thermal stress, by treating laser beam as heat source, and plastic stress by first assuming pure elastic stress in loading process, then obtaining true stress with kinematic hardening followed by the stress relaxation. The variance-based recursive method is applied to solve inverse problem by updating process parameters to match the measured mean residual stress. Three cutting parameters including depth of cut, feed per tooth, and cutting speed, and two laser parameters including laser-tool distance and laser power, are updated with respected to the minimization of resulting residual stress and measurement in each iteration. Experimental measurements are referred on the laser-assisted milling of Ti-6Al-4V grade 5 and ELI. The percentage difference between experiments and predictions is less than 5% for both materials, and the selection is completed within 50 loops.

Keywords: Inverse analysis; Iterative gradient search; Laser-assisted milling; Residual stress; Ti-6Al-4V

1. INTRODUCTION

The residual stress can largely affect the machined workpiece in terms of fatigue resistance. With the use of laser, higher temperature in shear zone softens the material potentially resulting in a shift of mean residual stress after laser-assisted milling [1], which significantly changes the damage tolerance and fatigue performance of product. Therefore, an inverse analysis is conducted on the mean residual stress after laser-assisted milling, in order to guide the selection of laser and cutting parameters based on the preferred mean residual stress. The forward problem, which is defined as the prediction of residual stress based on guessed process parameters, needs to be solved first. The methodology of solving forward problem in both conventional and laser-assisted milling has been studied through experiments [2-5] and numerical simulations [6, 7], but these methods have low efficiency when applied in inverse problem, which is defined as the prediction of process parameters for next iteration through iterative gradient search. Analytical models for residual stress in the conventional milling process have been validated for different materials [8-12]. However, when the effect of additional heat source by laser is considered, the microstructure evolution can be triggered and affect the residual stress. The overall forward problem methodology of the residual stress prediction considering laser effect is summarized in Fig.1. The heat source is calculated according to the size of laser spot and the laser power, and temperature field after laser preheating is calculated based on the conduction within workpiece [13, 14]. The geometry of milling tool is simplified as in orthogonal cutting at each instance, in order to predict the flow stress dependent on micro-

structure evolution [15, 16], followed by cutting forces [17] and machining temperature [18] predictions. The residual stress is then predicted through mechanical loading based on forces, thermal loading based on temperature, and relaxation [19].

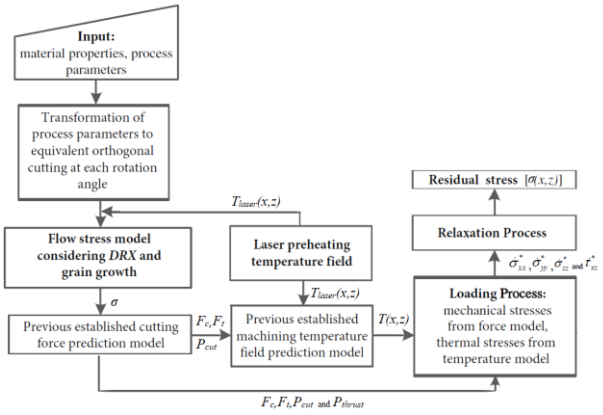

Fig. 1. Overall flow chart of forward predictive model.

Iterative gradient search method guesses the process parameters based on the difference between predicted target performance and experimental measurement. This procedure has been widely applied in inverse analysis of hydraulic parameters [20], material properties [21, 22], torque [23], and constitutive equation constants [24-26], due to relatively simplified forward problem. The predictions based on initial guesses are close to measurements, and the forward problem is solved by empirical model or numerical simulation within 10 iterations. However, the prediction of mean residual stress in laser-assisted milling is a complex procedure, which takes up to several days if solved by numerical simulation such as finite element analysis [16]. In addition, the resultant mean residual stress is very sensitive to cutting and laser parameters, and the predicted value could be far away from the measurement even though the initial guesses are close, which takes more iterations to locate the desired parameters. Therefore, a gain coefficient is included in the proposed model. The coefficient is able to speed up the progress if the initial gap is huge, and avoid convergence if the stopping criteria has not been reached, which enhances the computational efficiency and accuracy. Inverse analysis has been applied to satisfy residual stress [27, 28] but not mean residual stress requirements in laser-assisted milling. The inverse analysis method conducted in current study solves the forward problem through an analytical prediction model of mean residual stress in laser-assisted milling and includes a new iterative gradient search algorithm, which has been previously used by the authors on cutting force [29] and surface roughness [30], to solve the inverse problem. Three cutting parameters including depth of cut, feed per tooth, and cutting speed, and two laser parameters including laser-tool distance and laser power, are selected as process parameters. The analysis is conducted on measured mean residual stress after laser-assisted milling of Ti-6Al-4V alloy [31, 32].

2. Inverse Problem Methodology

In inverse analysis, iterative gradient search method is used to find desired target performance and corresponding process parameters [9]. After an initial guess X_0, depth of cut d_a, feed per tooth f_z, cutting speed V_r, laser-tool distance L, and laser power P are updated in each loop as

$$X_n = (d_a^n, f_z^n, V_r^n, L^n, P^n)^T \tag{1}$$

The process parameters in next loop are dependent on the gap between predicted and measured residual stress as

$$X_{n+1} = X_n + K_n(\bar{\sigma}_R^{\exp} - \bar{\sigma}_R^n)G \tag{2}$$

where $\bar{\sigma}_R^{\exp}$ is the mean residual stresses in machining and feed directions from experiments and $\bar{\sigma}_R^n$ is the mean residual stress predicted under X_n. The forward prediction of mean residual stress after laser-assisted milling has been proposed in previous works [33-35]. The mean residual stresses are calculated by averaging the residual stress profiles, which are predicted through the calculation of thermal stress, by treating laser beam as heat source, and plastic stress by first assuming pure elastic stress in loading process, then obtaining true stress with kinematic hardening followed by the stress relaxation. G is called gain coefficient, and K_n is called Kalman gain matrix [36-38] being updated in each loop as

$$K_n = P_n \left(\frac{\Delta \bar{\sigma}_R^{n-1}}{\Delta X_{n-1}} \right)^T R^{-1} \tag{3}$$

The error covariance matrix R is

$$R = \begin{pmatrix} \bar{\sigma}_{R,machining}^{\exp^2} & 0 \\ 0 & \bar{\sigma}_{R,feed}^{\exp^2} \end{pmatrix} \tag{4}$$

The derivative matrix $\left(\frac{\Delta \bar{\sigma}_R^{n-1}}{\Delta X_{n-1}} \right)^T$ is

$$\left(\frac{\Delta \bar{\sigma}_R^{n-1}}{\Delta X_{n-1}} \right) = \left(\frac{\bar{\sigma}_R^n - \bar{\sigma}_R^{n-1}}{d_a^n - d_a^{n-1}}, \frac{\bar{\sigma}_R^n - \bar{\sigma}_R^{n-1}}{f_z^n - f_z^{n-1}}, \frac{\bar{\sigma}_R^n - \bar{\sigma}_R^{n-1}}{V_r^n - V_r^{n-1}}, \frac{\bar{\sigma}_R^n - \bar{\sigma}_R^{n-1}}{L^n - L^{n-1}}, \frac{\bar{\sigma}_R^n - \bar{\sigma}_R^{n-1}}{P^n - P^{n-1}} \right) \tag{5}$$

where $\Delta X_0 = X_0$ and $\Delta \bar{\sigma}_R^0 = \bar{\sigma}_R^0$. The simulation covariance matrix P_n has an initial value of

Preprints (www.preprints.org) | NOT PEER-REVIEWED | Posted: 17 June 2019 doi:10.20944/preprints201906.0152.v1

Peer-reviewed version available at *Int. J. Adv. Manuf. Technol.* **2019**; doi:10.1007/s00170-019-04794-9

$$P_0 = \begin{pmatrix} (\Delta d_a)^2 & 0 & 0 & 0 & 0 \\ 0 & (\Delta f_z)^2 & 0 & 0 & 0 \\ 0 & 0 & (\Delta V_r)^2 & 0 & 0 \\ 0 & 0 & 0 & (\Delta L)^2 & 0 \\ 0 & 0 & 0 & 0 & (\Delta P)^2 \end{pmatrix} \quad (6)$$

where Δd_a, Δf_z, ΔV_r, ΔL, and ΔP are the expected ranges of variance. P_n is updated in each loop as

$$P_n = P_{n-1} - P_{n-1}\left(\frac{\Delta\bar{\sigma}_R^{n-1}}{\Delta X_{n-1}}\right)^T \left(\frac{\Delta\bar{\sigma}_R^{n-1}}{\Delta X_{n-1}} P_{n-1}\left(\frac{\Delta\bar{\sigma}_R^{n-1}}{\Delta X_{n-1}}\right)^T + R\right)^{-1} \times \frac{\Delta\bar{\sigma}_R^{n-1}}{\Delta X_{n-1}} P_{n-1} \quad (7)$$

The gain coefficient G in Eq. (2) is

$$G = \frac{\sum(\bar{\sigma}_R^{\exp} - \bar{\sigma}_R^{n-1})}{\sum(\bar{\sigma}_R^{n-1} - \bar{\sigma}_R^{n-2})} \quad (8)$$

The denominator of G avoids local convergence if the stopping criteria has not been reached. The numerator of G speeds up the gradient search process when the difference between measurement and guess is large, which enhances computational efficiency. Therefore, the proposed new iterative gradient search method is able to avoid convergence, more adaptive, and more robust. Both forward and inverse problems are solved analytically in one algorithm summarized in Fig.2.

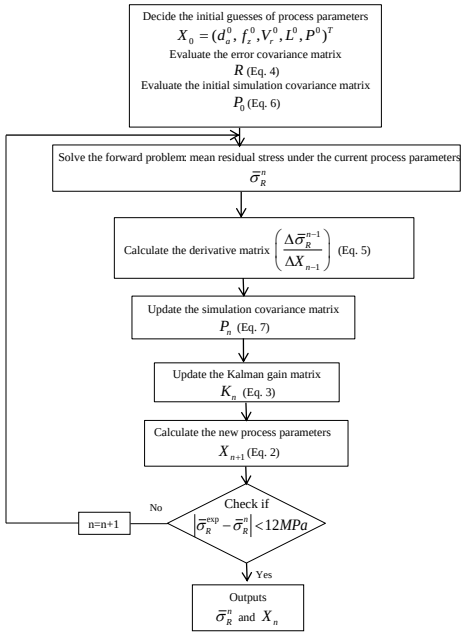

Fig. 2. Flow chart of the inverse analysis process.

3. Experimental Validation and Estimation of Residual Stress Via Inverse Problem

Experimental measurements are referred on laser-assisted milling of Ti-6Al-4V grade 5 and grade 23 (ELI) [31, 32] for validation of inverse analysis. The spindle rotation speed is 1253*RPM*. The size of laser spot is 2.5*mm* x 3.6*mm*, the laser power P is 185*W*, and the laser-tool distance L is 3.5*mm*. For milling tool, the rake angle is 15°, the diameter is 19.05*mm*, and the nose radius is 0.8*mm*. The cutting speed is 75*m/min*, the feed per tooth is 0.1*mm/tooth*, the axial depth of milling is 1*mm*, and the radial width of cut is 3*mm*.

The constitutive model of Ti-6Al-4V for flow stress prediction is

$$\sigma = (A_{hp} + K_{hp} d^{-0.5} + B\bar{\varepsilon}^n)(1 + C\ln\frac{\dot{\bar{\varepsilon}}}{\dot{\bar{\varepsilon}}_0})\{1 - (\frac{T - T_0}{T_m - T_0})^m\} \quad (9)$$

where T_m is melting temperature. All constitutive model parameters are listed in Table 1 [34], and d_0 is decided to be 10μm.

Table 1. Constitutive model parameters for Ti-6Al-4V.

Ti-6Al-4V Grade 5	A_{hp}(MPa)	K_{hp}(MPa $\sqrt{\mu m}$)	B(MPa)	C
	803.22	401.61	653.1	0.015
	m	n	T_m(°C)	$\dot{\bar{\varepsilon}}_0$ (s^{-1})
	0.6	0.45	1668	1
Ti-6Al-4V ELI	A_{hp}(MPa)	K_{hp}(MPa $\sqrt{\mu m}$)	B(MPa)	C
	803.22	401.61	653.1	0.025
	m	n	T_m(°C)	$\dot{\bar{\varepsilon}}_0$ (s^{-1})
	0.8	0.45	1630	1

For Ti-6Al-4V grade 5, the measured mean residual stress as well as prediction from inverse analysis in laser-assisted milling are shown in Fig.3. Measurements are collected every 50μm up to 200μm depth and averaged for mean residual stress. The initial guesses for inverse analysis are cutting depth of 1*mm*, feed per tooth of 0.22*mm/s*, cutting speed of 2.75*m/s*, laser-tool distance of 7.7*mm*, and laser power of 1034*W*. In machining direction, the mean residual stress from experiments is 191*MPa* in compression, and the prediction through inverse analysis is -182.72*MPa*. A close match is found after 44 iterations with a percentage difference of 4.33% as listed in Table 2. In feed direction, the mean residual stress from exper-

iments is 130.2*MPa* in compression, and the prediction through inverse analysis is -132.80*MPa* with a percentage difference of 1.99%. The process parameters in final iteration are cutting depth of 0.79*mm*, feed per tooth of 0.11*mm/s*, cutting speed of 1.62*m/s*, laser-tool distance of 6.03*mm*, and laser power of 816.6*W*. As observed in Fig.3, the proposed algorithm is able to jump out of local extreme several times throughout the inverse analysis until the stopping criteria are reached.

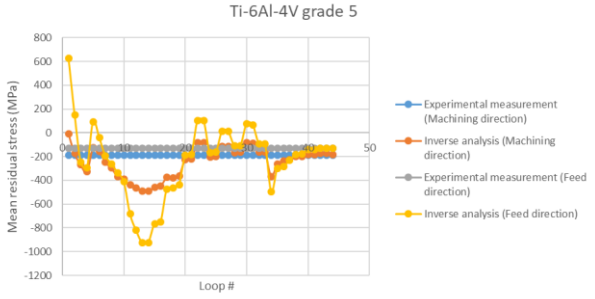

Fig. 3. Estimation of mean residual stress via inverse analysis on Ti-6Al-4V grade 5.

Table 2. Comparison of mean residual stress between experimental measurements and predictions through inverse analysis.

	Ti-6Al-4V Grade 5		
	Measured mean residual stress (*MPa*)	Prediction from inverse analysis (*MPa*)	Percentage difference (%)
Machining direction	-191	-182.72	4.33
Feed direction	-130.2	-132.80	1.99
	Ti-6Al-4V ELI		
	Measured mean residual stress (*MPa*)	Prediction from inverse analysis (*MPa*)	Percentage difference (%)
Machining direction	-175	-171.50	2.00
Feed direction	-143.5	-146.68	2.21

The measured mean residual stress as well as prediction from inverse analysis in laser-assisted milling of Ti-6Al-4V ELI are shown in Fig.4. The initial guesses for inverse analysis are cutting depth of 1*mm*, feed per tooth of 0.1*mm/s*, cutting speed of 1.25*m/s*, laser-tool distance of 3.5*mm*, and laser power of 70*W*. In machining direction, the mean residual stress from experiments is 175*MPa* in compression, and the prediction through inverse analysis is -171.5*MPa*. A close match is found after 27 iterations with a percentage difference of 2% as listed in Table 2. In feed direction, the mean residual stress from experiments is 143.5*MPa* in compression, and the prediction through inverse analysis is -146.68*MPa* with a percentage difference of 2.21%. The process parameters in final iteration are cutting depth of 0.51*mm*, feed per tooth of 0.06*mm/s*, cutting speed of 0.74*m/s*, laser-tool distance of 1.78*mm*, and laser power of 237.37*W*. Again, the proposed inverse analysis method is able to reach both high computational efficiency and accuracy.

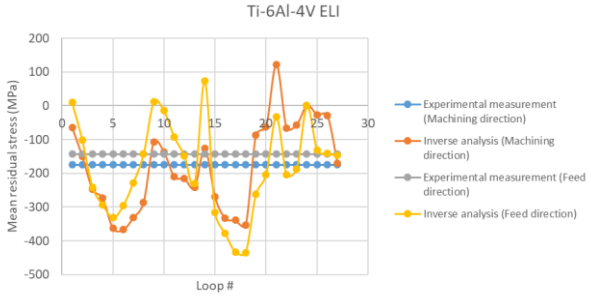

Fig. 4. Estimation of mean residual stress via inverse analysis on Ti-6Al-4V ELI.

When comparing the process parameters in final loop to initial guesses and experimental values, it is observed that although the process parameters are relatively close to initial guesses, they may be very different than experimental process parameters since the mean residual stress solutions may not be unique. In addition, the model-predicted residual stresses under experimental process parameters have been calculated by solving forward problem only [35]. The percentage errors for Ti-6Al-4V grade 5 and ELI are higher than 10% in both directions, which also indicates that the proposed inverse analysis method is highly accurate as the errors are mainly from the forward model.

4. Conclusions

An inverse analysis is conducted on the mean residual stress in laser-assisted milling which solves the forward problem of predicting residual stress based on guessed process parameters and the inverse problem of finding process parameters for next iteration by applying iterative gradient search. For forward problem, residual stress is affected by material recrystallization under laser effect. The laser beam is treated as a heat source on top. The milling tool geometry and process parameters are recalculated in orthogonal cutting. The recrystallization and grain growth are described by calibrated models showing the dependency of strain, strain rate, and temperature

on recrystallization. For the loading process, the elastic stresses are first predicted, and the real stresses are calculated considering kinematic hardening. The mean residual stress is then predicted after the stress relaxation. The variance-based recursive method is applied to solve inverse problem and update process parameters to match the measurements. Three cutting parameters including depth of cut, feed per tooth, and cutting speed, and two laser parameters including laser-tool distance and laser power, are updated in each iteration. The proposed iterative gradient search method introduces the gain coefficient that updates the parameters according to the difference between measurement and prediction, as well as the differences of predicted mean residual stress over loops, which makes the model able to avoid convergence, more adaptive, and more robust. The proposed model is validated through experimental measurements on the laser-assisted milling of Ti-6Al-4V grade 5 and ELI. The percentage difference between experiments and predictions is less than 5%, and the process is completed within 50 loops. Therefore, the proposed inverse analysis model is also highly accurate, and computationally efficient. The selected process parameters may be very different than experimental process parameters due to the multiple solutions issue. In addition, when comparing the model-predicted residual stresses under experimental process parameters to measurements, it is concluded that the errors are mainly from the forward model.

The proposed inverse analysis is the first approach to satisfy mean residual stress requirement after laser-assisted milling, which provides a reliable reference for the selection of process parameters when desirable mean residual stress is needed.

ACKNOWLEDGMENT

This work was supported by the Metal Industries Research and Development Centre (MIRDC), Kaohsiung, Taiwan

NOMENCLATURE

d_a : Axial depth of milling

f_z : Feed per tooth

G : Gain coefficient

K_n : Kalman gain matrix

L : Laser-tool distance

P : Laser power

P_n : Simulation covariance matrix

R : Error covariance matrix

T_m : Melting temperature

V_r : Cutting speed

REFERENCES

[1] Feng, Y., et al., *Analytical and Numerical Predictions of Machining-Induced Residual Stress in Milling of Inconel 718 Considering Dynamic Recrystallization.* 2018(51388): p. V004T03A023.

[2] Schlauer, C., R.L. Peng, and M. Odén, *Residual Stresses in a Nickel-Based Superalloy Introduced by Turning.* Materials Science Forum, 2002. **404-407**: p. 173-178.

[3] Dudzinski, D., et al., *A review of developments towards dry and high speed machining of Inconel 718 alloy.* International Journal of Machine Tools & Manufacture, 2004. **44**: p. 439-456.

[4] Sharman, A.R.C., J.I. Hughes, and K. Ridgway, *An analysis of the residual stresses generated in Inconel 718™ when turning.* Journal of Materials Processing Technology, 2006. **173**(3): p. 359-367.

[5] Madariaga, A., et al., *Analysis of residual stress and work-hardened profiles on Inconel 718 when face turning with large-nose radius tools.* The International Journal of Advanced Manufacturing Technology, 2014. **71**(9-12): p. 1587-1598.

[6] Outeiro, J.C., et al., *Analysis of residual stresses induced by dry turning of difficult-to-machine materials.* CIRP Annals - Manufacturing Technology, 2008. **57**(1): p. 77-80.

[7] Le Coz, G., et al., *Residual stresses after dry Machining of Inconel 718, experimental results and numerical simulation.* 2010.

[8] Ulutan, D., B. Erdem Alaca, and I. Lazoglu, *Analytical modelling of residual stresses in machining.* Journal of Materials Processing Technology, 2007. **183**(1): p. 77-87.

[9] Fergani, O., et al., *Analytical modeling of residual stress and the induced deflection of a milled thin plate.* The International Journal of Advanced Manufacturing Technology, 2014. **75**(1-4): p. 455-463.

[10] Peng, F.Y., et al., *Analytical modeling and experimental validation of residual stress in micro-end-milling.* The International Journal of Advanced Manufacturing Technology, 2016. **87**(9-12): p. 3411-3424.

[11] Zhou, R. and W. Yang, *Analytical modeling of residual stress in helical end milling of nickel-aluminum bronze.* The International Journal of Advanced Manufacturing Technology, 2016. **89**(1-4): p. 987-996.

[12] Huang, X., X. Zhang, and H. Ding, *An Enhanced Analytical Model of Residual Stress for Peripheral Milling.* Procedia CIRP, 2017. **58**: p. 387-392.

[13] Pan, Z., et al., *Heat affected zone in the laser-assisted milling of Inconel 718.* Journal of Manufacturing Processes, 2017. **30**: p. 141-147.

[14] Feng, Y., et al., *Analytical prediction of temperature in laser-assisted milling with laser preheating and machining effects.* The International Journal of Advanced Manufacturing Technology, 2018.

[15] Pan, Z., Y. Feng, and S.Y. Liang, *Material microstructure affected machining: a review.* Manufacturing Review, 2017. **4**: p. 5.

[16] Pan, Z., et al., *Microstructure-sensitive flow stress modeling for force prediction in laser assisted milling of Inconel 718.* Manufacturing Review, 2017. **4**: p. 6.

[17] Pan, Z., et al., *Force modeling of Inconel 718 laser-assisted end milling under recrystallization effects.* The International Journal of Advanced Manufacturing Technology, 2017. **92**(5): p. 2965-2974.

[18] Feng, Y., Z. Pan, and S.Y. Liang, *Temperature prediction in Inconel 718 milling with microstructure evolution.* The International Journal of Advanced Manufacturing Technology, 2018. **95**(9-12): p. 4607-4621.

[19] Pan, Z., et al., *Turning induced residual stress prediction of AISI 4130 considering dynamic recrystallization.* Machining Science and Technology, 2017. **22**(3): p. 507-521.

[20] Song, X., et al., *Numerical Comparison of Iterative Ensemble Kalman Filters for Unsaturated Flow Inverse Modeling.* Vadose Zone J., 2013.

[21] Gua, Y., et al., *Micro-indentation and inverse analysis to characterize elastic-plastic graded materials.* Materials Science and Engineering, 2003. **A345**: p. 223-233.

[22] Xie, T., et al., *An inverse analysis to estimate the endothermic reaction parameters and physical properties of aerogel insulating material.* Applied Thermal Engineering, 2015. **87**: p. 214-224.

[23] Cuellar, K.J.Q. and J.L.L. Silveira, *Analysis of Torque in Friction Stir Welding of Aluminum Alloy 5052 by Inverse Problem Method.* Journal of Manufacturing Science and Engineering, 2017. **139**.

[24] Agmell, M., A. Ahadi, and J.-E. Ståhl, *Identification of plasticity constants from orthogonal cutting and inverse analysis.* Mechanics of Materials, 2014. **77**: p. 43-51.

[25] Denkena, B., et al., *Inverse Determination of Constitutive Equations and Cutting Force Modelling for Complex Tools Using Oxley's Predictive Machining Theory.* Procedia CIRP, 2015. **31**: p. 405-410.

[26] Ning, J., et al., *Inverse determination of Johnson–Cook model constants of ultra-fine-grained titanium based on chip formation model and iterative gradient search.* The International Journal of Advanced Manufacturing Technology, 2018. **99**: p. 1131–1140.

[27] Faghidian, S.A., *Inverse determination of the regularized residual stress and eigenstrain fields due to surface peening.* J Strain Analysis, 2015. **50**(2): p. 84-91.

[28] Buljak, V., et al., *Estimation of residual stresses by inverse analysis based onexperimental data from sample removal for "small punch" tests.* Engineering Structures, 2017. **136**: p. 77-86.

[29] Feng, Y., et al., *Inverse analysis of the cutting force in laser-assisted milling on Inconel 718.* The International Journal of Advanced Manufacturing Technology, 2018. **96**(1): p. 905-914.

[30] Feng, Y., et al., *Inverse Analysis of Inconel 718 Laser-Assisted Milling to Achieve Machined Surface Roughness.* International Journal of Precision Engineering and Manufacturing, 2018. **19**(11): p. 1611-1618.

[31] Hedberg, G.K., *Laser assisted milling of difficult to machine materials*. 2013, Purdue University.

[32] Hedberg, G.K. and Y.C. Shin, *Laser Assisted Milling of Ti-6Al-4V ELI with the Analysis of Surface Integrity and its Economics.* Lasers in Manufacturing and Materials Processing, 2015. **2**(3): p. 164-185.

[33] Pan, Z., et al., *Turning Force Prediction of AISI 4130 Considering Dynamic Recrystallization.* 2017(50725): p. V001T02A040.

[34] Pan, Z., et al., *Prediction of machining-induced phase transformation and grain growth of Ti-6Al-4 V alloy.* The International Journal of Advanced Manufacturing Technology, 2016. **87**(1-4): p. 859-866.

[35] Feng, Y., et al., *Residual stress prediction in laser-*

assisted milling considering recrystallization effects. The International Journal of Advanced Manufacturing Technology, 2019.

[36] Mirkoohi, E., Bocchini, P., and Liang, S.Y., *An analytical modeling for process parameter planning in the machining of Ti-6Al-4V for force specifications using an inverse analysis.* The International Journal of Advanced Manufacturing Technology, 2018. **98**: p. 2347.

[37] Mirkoohi, E., Bocchini, P., and Liang, S.Y., *Inverse analysis of residual stress in orthogonal cutting.* Journal of Manufacturing Processes, 2019. **38**: p. 462-471.

[38] Mirkoohi, E., Bocchini, P., and Liang, S.Y. *An Analytical Modeling for Designing the Process Parameters for Temperature Specifications in Machining*. *Preprints* **2018**, 2018070528

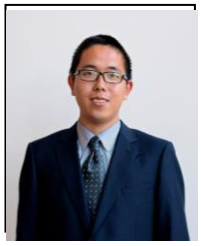

AUTHOR INFORMATION

Yixuan Feng is a Ph.D. candidate in the George W. Woodruff School of Mechanical Engineering, Georgia Institute of Technology, Atlanta, Georgia, United States. His research interest is laser-assisted milling.